HHS Public Access

Author manuscript

Psychiatry Res. Author manuscript; available in PMC 2018 March 30.

Published in final edited form as:

Psychiatry Res. 2017 March 30; 261: 72–74. doi:10.1016/j.pscychresns.2017.01.006.

Using probabilistic tractography to target the subcallosal cingulate cortex in patients with treatment resistant depression

Evangelia Tsolaki[a], **Randall Espinoza**[b,c], and **Nader Pouratian**[a,d]

[a]Department of Neurosurgery, David Geffen School of Medicine at UCLA, Los Angeles, CA, USA

[b]Department of Psychiatry and Biobehavioral Sciences, David Geffen School of Medicine at UCLA, Los Angeles, CA, USA

[c]Semel Institute for Neuroscience and Human Behavior, David Geffen School of Medicine at UCLA, Los Angeles, CA, USA

[d]Brain Research Institute, David Geffen School of Medicine at UCLA, Los Angeles, CA, USA

1. Introduction

While some studies of deep brain stimulation (DBS) for treatment resistant depression (TRD) suggest benefit (Mayberg et al., 2005; Bergfeld et al., 2016), a randomized controlled trial of subcallosal cingulate cortex (SCC) DBS for TRD was halted due to a low likelihood of success (Morishita et al., 2014). Aberrant targeting may contribute to suboptimal outcomes. Identifying the essential area to stimulate within SCC remains a significant challenge. Given the network-basis of depression, the target likely involves the convergence of white matter tracts implicated in multiple disease-related circuits (Lujan et al., 2012; Riva-Posse et al., 2014). However, this approach has not been validated beyond a single institution (Riva-Posse et al., 2014). Moreover, a data-driven methodology to define the optimal target and provide a tomographic map to guide targeting and programming does not exist for SCC although it has been reported in essential tremor and chronic pain (Pouratian et al., 2011; Kim et al., 2016). We report a novel approach using probabilistic tractography to delineate patient-specific tomographic maps for SCC DBS for TRD.

2. Methods

Two subjects with TRD who underwent bilateral SCC DBS implantation as part of a DBS for TRD trial were evaluated clinically and radiographically. IRB approval and informed consent were obtained. Implantation was done blind of tractography results. Before surgery, each subject underwent 3T magnetic resonance imaging, including high resolution T1-

Correspondence to: Department of Neurosurgery, University of California, Los Angeles, Neuroscience Research Building 225, Los Angeles, CA 90095, USA.

Conflict of interest

Dr Pouratian holds a patent related to using tractography for targeting of deep brain stimulation.

Contribution

Study concept, design, analysis, and drafting of manuscript: Tsolaki, Pouratian

Critical revision of the manuscript: Tsolaki, Pouratian, Espinoza

weighted anatomical images (TR 11ms, TE 2.81ms, flip angle 20°, 0.9375 mm isotropic voxels, and 192 slices) and single shot spin echo echo planar imaging for diffusion tensor imaging (TR 9200ms, TE 87ms, 2 mm isotropic voxels, b value=1000, and 20 directions). Post-operative computed tomography (CT) (0.6mm slice thickness and 0.48mm voxel size) of the head was acquired to assess lead position. T1 images were skull stripped (BET) (Smith 2002), segmented (Zhang et al., 2001) and registered to MNI152 template (FLIRT-FNIRT) (Jekinson et al., 2002). Eddy current correction was applied to diffusion data before skull extraction and then a multifiber diffusion model was fitted on the data (Behrens et al., 2007).

We used FSL probabilistic tractography (5000 samples, 0.2 curvature threshold, loopcheck termination, 2000 maximum number of steps, 0.5 mm step length and 0.01 subsidary fibre fraction threshold) to initially delineate the connectivity of anatomically-defined SCC (Gutman et al., 2009) with the entire brain. Then, for each predefined target area (Figure 1A, bilateral medial prefrontal cortices via forceps minor and uncinate fasciculus, ipsilateral ventral striatum and anterior cingulate), we identify voxels with the maximum probability of connectivity with the anatomically-defined SCC. We then use the coordinates of these voxels as subject-specific targets for subsequent delineation of TOT within SCC. We then determined the probability of connectivity of each SCC voxel with each of the connectivity-determined patient-specific targets using them as waypoint, termination and classification masks. The SCC probability maps for each target were then smoothed using a Gaussian kernel (2mm, to account for stimulation spread), multiplied on a pixel-by-pixel basis and high pass filtered in order to include only voxels with at least 10% of the maximum joint probability. The resulting conjunction probability map identified the region within SCC with the highest probability of connectivity with all four targets, herein referred to as the tractography-guided optimized target (TOT).

The volume of activated tissue was estimated using programming parameters (frequency 130Hz, pulse width 91ms and amplitude 8mA, maximal volume diameter 8 mm) and was defined on postoperative CT in a manner similar to that described by Accolla and colleagues (Accolla et al., 2016), with a final total seed volume of 288mm^3. The whole brain connectivity of the estimated volume of activated tissue was explored and the distance between the TOT and activated tissue was calculated. Finally, we quantified the probability of connectivity of each seed (TOT, estimated volume of activated tissue) with each target based on the number of streamlines between each seed and target.

3. Results

One subject was a responder while the other was not (MADRS decreased by 31 (84% change) and 3 (8% change), respectively). In both subjects, SCC was structurally connected with all four targets (Figure 1A). Despite the probability of connectivity of each SCC voxel being distinct for each target (Figure 1B), a SCC subregion with the highest joint probability of connectivity with all 4 targets was identified in each hemisphere (TOT, Figure 1C). In the responder, the pair of contacts used (2 and 3) for stimulation were on average closer to TOT than other pair of contacts (*Left_Hemisphere*: Contact1=4.6mm, Contact2_active=3.01mm, Contact3=1.84mm, Contact4=2.69mm, *Right Hemisphere*: Contact1=4.34mm,

Contact2=3.84mm, Contact3=4.34mm, Contact4=5.56mm) whereas in the non-responder, the contact pairs used for stimulation (2 and 3) were further from TOT than other contact pairs (e.g., 1 and 2) (*Left Hemisphere*: Contact1=2.45mm, Contact2=2.45mm, Contact3=4.24mm, Contact4=5.84mm, *Right Hemisphere*: Contact1=2.69mm, Contact2=2.69mm, Contact3=3.90mm, Contact4=5.58mm).

The structural connectivity of estimated volume of activated tissue in the responder demonstrated connectivity with all four targets, whereas in the non-responder, there was <1% probability of connectivity with the ventral striatum (Figure 1D). In the non-responder, selection of contacts closer to TOT resulted in connectivity with all targets, but the patient opted to be explanted before this hypothesis could be tested. In both subjects, the probability of connectivity (i.e., number of streamlines per seed voxel) with each of the four target regions bilaterally was 4.82 times higher for TOT compared to the original site of stimulation.

4. Discussion

We provide additional confirmation of the value of tractography to identify the optimal site of stimulation for SCC DBS for TRD (Riva-Posse et al., 2014). Rather than relying on a manual, iterative, and deterministic methodology, the proposed method defines a novel data-driven probabilistic TOT. The method is supported by results that demonstrate that stimulation was delivered at the contacts closest to TOT in the responder whereas in the non-responder, the stimulation contacts were more distant from TOT. This approach assumes that each tract is equally weighted, although other reports suggest particular tracts (such as mPFC) may be of greater important (Accolla et al., 2016). Further studies with more than 2 subjects will be needed to define the value of these tomographic maps for predicting response to DBS, to identify potentially superior active therapeutic contacts, and to evaluate the optimal weighting of these probability-based maps.

Regarding the tractography methods, previous methods are based on iterative deterministic assessments, which is prone to sampling limitations (Avecillas-Chasin et al., 2015; Choi et al., 2015). While the probabilistic approach is time intensive, the data-driven nature may be more practical and provide advantages over a manual iterative approach. Moreover, probabilistic tractography provides more consistent and plausible tractography results that deterministic tractography (Petersen et al., 2016). Still, there are studies that controvert the reliability of diffusion tractography, whether using deterministic or probabilistic methods, for reproducing known anatomy, with results highly dependent on data quality, the algorithm selected, and the parameter settings (Thomas et al., 2014; Knösche et al., 2015). However, tractography is the only available tool to non-invasively evaluate white-matter microstructure and to address the clinical need for white matter pathways characterization (Basser et al., 2014). Moreover, even if it is not reliable at precisely reproducing known anatomy, these methods can still theoretically provide usable biomarkers to guide neuromodulation, as suggested here.

This novel method offers an automated and patient-specific approach to provide tomographic maps that could be used clinically in an intuitive fashion for DBS targeting and

programming. The encouraging preliminary results encourage further exploration of this novel method for optimizing SCC targeting. The main limitation of this study is the small number of patients and estimates of tissue activation. Because DBS for TRD remains investigational and new implants are limited, we must optimize opportunities to learn from previously implanted subjects in order to advance the field.

Acknowledgments

Dr Pouratian is supported NIBIB K23EB014236 and philanthropic support the Casa Colina Centers for Rehabilitation.

References

Accolla EA, Aust S, Merkl A, Schneider GH, Kühn AA, Bajbouj M, et al. Deep brain stimulation of the posterior gyrus rectus region for treatment resistant depression. Journal of Affective Disorders. 2016; 194:33–37. [PubMed: 26802505]

Avecillas-Chasin JM, Alonso-Frech F, Parras O, del Prado N, Barcia JA. Assessment of a method to determine deep brain stimulation targets using deterministic tractography in a navigation system. Neurosurg Rev. 2015; 38:739–750. [PubMed: 25962557]

Basser PJ, Özarslan E. Chapter 1 – Introduction to Diffusion MR BT – Diffusion MRI (Second). 2014:3–9.

Behrens TEJ, Berg HJ, Jbabdi S, Rushworth MFS, Woolrich MW. Probabilistic diffusion tractography with multiple fibre orientations: what can we gain? NeuroImage. 2007; 34(1):144–155. [PubMed: 17070705]

Bergfeld IO, Mantione M, Hoogendoorn MC, Ruhé HG, Notten P, van Laarhoven J, et al. Deep brain stimulation of the ventral anterior limb of the internal capsule for treatment-resistant depression: a randomized clinical trial. JAMA Psychiatry. 2016; 73:456–464. [PubMed: 27049915]

Choi KS, Riva-Posse P, Gross RE, Mayberg HS. Mapping the “depression switch” during intraoperative testing of subcallosal cingulate deep brain stimulation. JAMA Neurol. 2015; 72:1252–1260. [PubMed: 26408865]

Gutman DA, Holtzheimer PE, Behrens TEJ, Johansen-Berg H, Mayberg HS. A tractography analysis of two deep brain stimulation white matter targets for depression. Biological Psychiatry. 2009; 65:276–282. [PubMed: 19013554]

Jenkinson M, Bannister P, Brady M, Smith S. Improved optimization for the robust and accurate linear registration and motion correction of brain images. NeuroImage. 2002; 17(2):825–841. [PubMed: 12377157]

Kim W, Chivukula S, Hauptman J, Pouratian N. Diffusion tensor imaging-based thalamic segmentation in deep brain stimulation for chronic pain conditions. Stereotac Funct Neurosurg. 2016; 94:225–234.

Knösche TR, Anwander A, Liptrot M, Dyrby TB. Validation of tractography: Comparison with manganese tracing. Human Brain Mapping. 2015; 36:4116–4134. [PubMed: 26178765]

Lujan JL, Chaturvedi A, Malone DA, Rezai AR, Machado AG, McIntyre CC. Axonal pathways linked to therapeutic and nontherapeutic outcomes during psychiatric deep brain stimulation. Hum Brain Mapp. 2012; 33:958–68. [PubMed: 21520343]

Mayberg HS, Lozano AM, Voon V, McNeely HE, Seminowicz DA, Hamani C, Schwalb JM, Kennedy SH. Deep brain stimulation for treatment-resistant depression. Neuron. 2005; 45:651–660. [PubMed: 15748841]

Morishita T, Fayad SM, Higuchi MA, Nestor KA, Foote KD. Deep brain stimulation for treatment-resistant depression: systematic review of clinical outcomes. Neurotherapeutics. 2014; 11:475–84. [PubMed: 24867326]

Petersen MV, Lund TE, Sunde N, Frandsen J, Rosendal F, Juul N, Østergaard K. Probabilistic versus deterministic tractography for delineation of the cortico-subthalamic hyperdirect pathway in patients with Parkinson disease selected for deep brain stimulation. J Neurosurg. 2016; 8:1–12.

Pouratian N, Zheng Z, Bari AA, Behnke E, Elias WJ, Desalles AA. Multi-institutional evaluation of deep brain stimulation targeting using probabilistic connectivity-based thalamic segmentation. J Neurosurg. 2011; 115:995–1004. [PubMed: 21854118]

Riva-Posse P, Choi KS, Holtzheimer PE, McIntyre CC, Gross RE, Chaturvedi A, et al. Defining critical white matter pathways mediating successful subcallosal cingulate deep brain stimulation for treatment-resistant depression. Biological Psychiatry. 2014; 76:963–969. [PubMed: 24832866]

Smith SM. Fast robust automated brain extraction. Human Brain Mapping. 2002; 17(3):143–155. [PubMed: 12391568]

Thomas C, Ye FQ, Irfanoglu MO, Modi P, Saleem KS, Leopold DA, Pierpaoli C. Anatomical accuracy of brain connections derived from diffusion MRI tractography is inherently limited. Proceedings of the National Academy of Sciences. 2014; 111(46):16574–16579.

Zhang Y, Brady M, Smith S. Segmentation of brain MR images through a hidden Markov random field model and the expectation-maximization algorithm. IEEE Transactions on Medical Imaging. 2001; 20(1):45–57. [PubMed: 11293691]

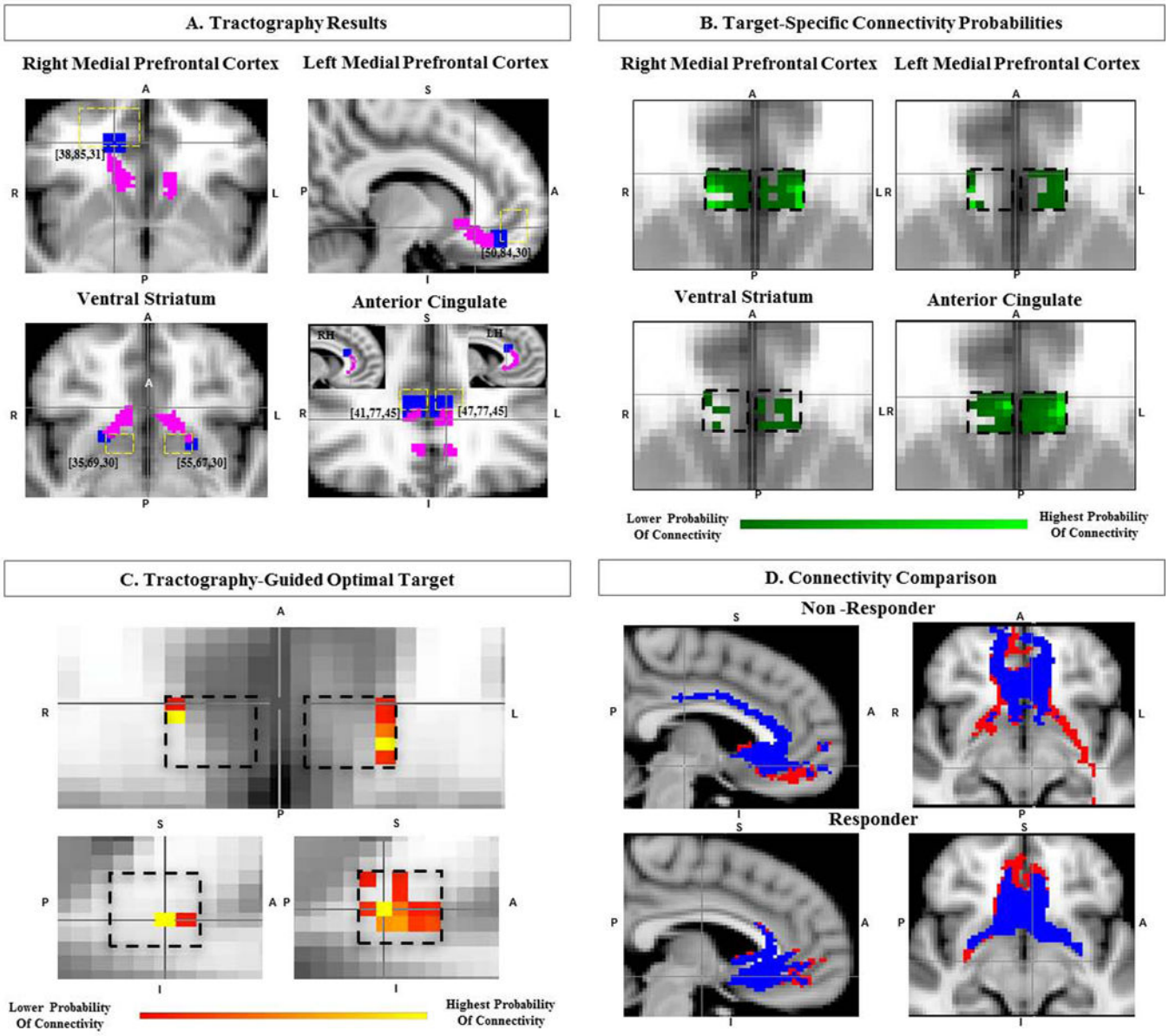

Figure 1.

Identifying the Connectivity-Guided Optimal Target within the Subcallosal Cingulate cortex (SCC) **A**. Single-subject structural connectivity (magenta) of SCC to 4 distinct subject specific target regions (blue), as labeled, with coordinates on MNI152 template (predefined ROI areas with yellow dashed lines). **B.** Single-subject tomographic target-specific probabilistic connectivity maps of SCC. **C**. Single-subject tractography-guided optimal target (TOT) within SCC (black dashed lines), identifying the region with highest joint probability of connectivity with all targets. **D**. Connectivity comparison of TOT (red) versus volume of activated tissue (blue) in both responder and non-responder, activated tissue connectivity with ventral striatum in the non-responder. A=anterior, P=posterior, R=right, L=left, S=superior, I=inferior, RH=Right Hemisphere, LH=Left Hemisphere.